

Mixing in a Meandering Jet: a Markovian Approximation

M. Cencini¹, G. Lacorata^{2,*}, A. Vulpiani¹ and E. Zambianchi³

November 6, 2018

¹ Dipartimento di Fisica, Università di Roma "la Sapienza"
Piazzale Aldo Moro 5, I-00185 Roma, Italy and
Istituto Nazionale Fisica della Materia, Unità di Roma

² Dipartimento di Fisica, Università dell' Aquila
Via Vetoio 1, I-67010 Coppito, L'Aquila, Italy

³ Istituto di Meteorologia e Oceanografia Istituto
Universitario Navale, Corso Umberto I 174, I-80138 Napoli, Italy.

* and Istituto di Fisica dell'Atmosfera - CNR
P.le Luigi Sturzo 31, I-00144 Roma, Italy

Abstract

In this paper we investigate mixing and transport in correspondence of a meandering jet. The large-scale flow field is a kinematically assigned streamfunction. Two basic mixing mechanisms are considered, first separately and then combined together: deterministic chaotic advection, induced by a time dependence of the flow, and turbulent diffusion, described by means of a stochastic model for particle motion.

Rather than looking at the details of particle trajectories, fluid exchange is studied in terms of markovian approximations. The two-dimensional physical space accessible to fluid particles is subdivided into regions characterized by different Lagrangian behaviours. From the observed transitions between regions it is possible to derive a number of relevant quantities characterizing transport and mixing in the

studied flow regime, such as residence times, meridional mixing, correlation functions. These estimated quantities are compared with the corresponding ones resulting from the actual simulations. The outcome of the comparison suggests the possibility of describing in a satisfactory way at least some of the mixing properties of the system through the very simplified approach of a first order markovian approximation, whereas other properties exhibit memory patterns of higher order.

Key words: Gulf Stream, mixing, chaotic advection, turbulent diffusion, Markov process.

PACS numbers: 92.10.Lq, 92.10.Fj, 05.45.+b

1 Introduction

Western boundary current extensions typically exhibit a meandering jet-like flow pattern. The most renowned example of this is given by the meanders of the Gulf Stream extension, which have been investigated in their variability by means of both hydrographic/currentmetric and remotely sensed data (see, e.g., Watts, 1983, for a survey of earlier studies; Halliwell and Mooers, 1983; Vazquez and Watts, 1985; Cornillon et al., 1986; Tracey and Watts, 1986; Kontoyiannis and Watts, 1994; Lee, 1994).

These strong currents often separate very different regions of the oceans, characterized by water masses which are quite different in terms of their physical and biogeochemical characteristics. Consequently, they are associated with very sharp and localized property gradients; this makes the study of mixing processes across them particularly relevant also for interdisciplinary investigations. This is the case of the Gulf Stream (Bower et al., 1985; Wishner and Allison, 1986; Bower and Lozier, 1994), of the Kuroshio and of the Brazil/Malvinas current (Backus, 1986).

The mixing properties of passive tracers across meandering jets has been investigated in the recent past by a number of authors, following essentially two different approaches. The first one is that of dynamical models, where the flow is produced by integrating the equations of motion, time dependence

is typically produced by (barotropic or baroclinic) instability processes, and dissipation is present (e.g., Yang, 1996). These models account for several mechanisms acting in mixing in the real ocean, even if sorting out single processes of interest may be sometimes tricky.

A second and simpler approach, the one followed in this paper, is that of kinematic models (Bower, 1991; Samelson, 1992; Dutkiewicz et al., 1993 – hereafter respectively referred to as B91, S92, DGO93 – Duan and Wiggins, 1996; for slightly different kinds of flows see also Lacorata et al., 1995). In such models the large-scale velocity field is represented by an assigned flow whose spatial and temporal characteristics mimic those observed in the ocean. However, the flow field may not be dynamically consistent in the sense of being a solution of the equations of motion, or of conserving, e.g., potential vorticity. Despite their somehow artificial character, these simplified models enable to focus on very basic mixing mechanisms.

The paper B91 represents a first attempt at understanding particle exchange in a two-dimensional meandering jet steadily propagating eastward.

The large-scale flow proposed in B91 has been utilized as a background field in further works where mixing is separately enhanced by two different transport mechanisms. S92 considers a modification of the B91 flow field where fluid exchange is induced by chaotic advection generated by a flow time dependence. The basic flow is made time-dependent in three different fashions: the superposition of a time-dependent meridional velocity; that of a propagating plane wave; a time oscillation of the meander amplitude, which is the case we further investigate in this paper.

The Melnikov method (see Lichtenberg and Lieberman 1992, LL92 hereafter) is used in S92 to explore the chaotic behaviour around the separatrices of the original B91 flow when a time dependence is added. One of the results of this investigation is that while mixing occurs between adjacent regions, over a broad range of the meander oscillation frequencies, it does not easily take place across the jet, i.e. from recirculations south of the jet to recirculations north of it. This is inherently due to the oscillation pattern of the large-scale velocity, and we will discuss this in detail further in this paper.

Particle exchange in the same B91 flow is achieved by DGO93 by superimposing to the original time-independent basic flow a stochastic term which describes mesoscale turbulent diffusion in the upper ocean. The focus of that paper is on the exchange among recirculations and jet core and viceversa, and on the homogenization processes in the recirculation. The numerical experi-

ments presented in DGO93 are carried out for quite short integration times, which do not allow for exploring the mixing across the jet.

Since in the real ocean the two above mixing mechanisms, i.e. chaotic advection and turbulent diffusion, are simultaneously present, in this paper we investigate how particle exchange varies through the progression from periodic to stochastic disturbances, revisiting and putting together the mixing processes studied by S92 and DGO93.

This is done by looking at particle statistics obtained by numerical computation of the trajectories of a large number of particles (or equivalently, since our system is ergodic, following one particle for a very long time) in three different flows: one equivalent to S92, in which mixing is induced by chaotic advection; one equivalent to DGO93, where it is due to turbulent diffusion, and a combination of them.

Dispersion processes in a flow field can be quantitatively characterized, in the Lagrangian description, in terms of different quantities, such as, e.g., the Lyapunov exponent λ (Benettin et al. 1980) and the diffusion coefficients D_{ij} (LL92).

However the above indicators, even if mathematically well defined, can be rather irrelevant for many purposes. The Lyapunov exponent is the inverse of a characteristic time t_L , related to the exponential growth of the distance between two trajectories initially very close; however, other characteristic time scales may appear and result as relevant in the description of a system, such as those involved in the correlation functions and in the mixing phenomena. It is worth stressing that there is not a clear relationship, if any, among these times and t_L .

Also the use of the diffusion coefficients can have severe limitations; sometimes the D_{ij} are not able to take into account the basic mechanisms of the spreading and mixing (Artale et al., 1997). Our western boundary current extension system has essentially a periodic structure in the zonal direction. It is thus possible to define and (numerically) compute the diffusion coefficients. They are related to the asymptotic behaviour, i.e. long times and large spatial scales, of a cloud of test particles. On the other hand, if one is interested in the meridional mixing, which takes place over finite time scales, the diffusion coefficients may not be very useful. In such situations it is then worthwhile to look for alternative methods of describing mixing processes, as was done by Artale et al. (1997) looking at dispersion in closed basins or by Buffoni et al. (1997), who employ exit times for the characterization of

transport in basins with complicated geometry.

Our investigation is carried out with a non conventional approach, in a geophysical contest, as we try to analyze the system from the standpoint of the approximation in terms of markovian processes (Cecconi and Vulpiani 1995, Kluiving et al 1992, Nicolis et al. 1997, Fraedrich and Müller 1983 and Fraedrich 1988).

We start from the consideration that the flow field we want to characterize in terms of fluid transport can be subdivided into regions corresponding to different lagrangian behaviours: ballistic fly in the meandering jet core, trapping inside recirculations, retrograde motion in the far field. As an obvious consequence, we introduce a partition of the two-dimensional physical space accessible to fluid particles and divide it into these disjoint regions selected in a natural way by the dynamics. At this point, one can study the transition of fluid particles between different regions as a discrete stochastic process generated by the dynamics itself.

In this paper we study the statistical properties of this stochastic process and we compare it with an approximation in terms of Markov chains. For some fluid exchange properties — such as, e.g., the probability distribution of the particle exit times from the jet or from the neighbouring recirculation regions — the effects of the two different mixing mechanisms and the results of the markovian approximation are very similar. Other properties, such as the meridional mixing across the jet, do not show such an obvious possibility to be described in terms of markovian simple processes. However, for those properties the markovian description is seen to be relatively more accurate in the case when chaotic advection and turbulent diffusion are simultaneously present.

The comparison between the results of the numerical simulations and those computed in the markovian approximation allows for a deeper understanding of the transport and mixing mechanisms.

In section 2 we introduce the kinematic model for the flow field correspondent to the Gulf Stream flow and both models for chaotic advection and turbulent diffusion. Section 3 is devoted to the description of the markovian approximation. In Section 4 we discuss the numerical results and the comparison of the true dynamics with the markovian approximation. Section 5 contains some discussion and conclusions. The Appendix summarizes some basic properties of Markov chains.

2 The flow field

The large-scale flow in its basic form, representing the velocity field in correspondence of a meandering jet, is the same introduced in B91 and further discussed in S92; in a fixed reference frame the streamfunction is given by

$$\psi(x', y', t) = \psi_0 \left[1 - \tanh \frac{y' - A \cos \kappa(x' - c_x t)}{\lambda(1 + k^2 A^2 \sin^2 \kappa(x' - c_x t))^{1/2}} \right] \quad (1)$$

where ψ_0 represents half of the total transport, A , k and c_x the amplitude, wavenumber and phase speed of the pattern. A change of coordinates into a reference frame moving eastward with a velocity coinciding with the phase speed c_x , and a successive nondimensionalization, yield a streamfunction as follows:

$$\phi = -\tanh \left[\frac{y - B \cos kx}{(1 + k^2 B^2 \sin^2 kx)^{1/2}} \right] + cy \quad (2)$$

The relationship between variables in (1) and (2) is given by (see S92):

$$x \equiv \frac{x' - c_x t}{\lambda}, \quad y \equiv y'/\lambda, \quad B \equiv A/\lambda$$

$$\phi \equiv \frac{\psi}{\psi_0} + cy, \quad c \equiv \frac{c_x L}{\psi_0}, \quad \kappa \equiv k\lambda$$

The evolution of the tracer particles is given by:

$$\frac{dx}{dt} = -\frac{\partial \phi}{\partial y}, \quad \frac{dy}{dt} = \frac{\partial \phi}{\partial x}. \quad (3)$$

The natural distance unit for our system is given by the jetwidth λ , set to 40 Km (B91, S92). The basic flow configuration is very similar to case (b) of B91: B was chosen as 1.2; c as 0.12. The only sensible difference is the value assigned to L , i.e. the meander wavelength, which was set as 7.5, as will be discussed below.

In fig. 1 we show the stationary velocity vector field in the moving frame: the field is evidently divided into three very different flow regions (see also B91, S92, DGO93): the central, eastward moving jet stream, recirculation regions north and south of it, and a far field; the far field, given our choice of parameters, appears to be moving westward at a phase speed of $-c_x \equiv -0.12$.

This intrinsic self subdivision of the flow field will result crucial for building a partition of the possible states available to our test particles, which will be investigated in markovian terms.

Chaotic advection may be induced in a two-dimensional flow field by introducing a time dependence (see e.g. Crisanti et al., 1991). This is simply achieved by adding to the basic steady flow some typically small perturbation which varies in time. Among three basic mechanisms discussed by S92, we chose here a time-dependent oscillation of the meander amplitude:

$$B(t) = B_0 + \epsilon \cdot \cos(\omega t + \theta) \quad (4)$$

In (4) we set $B_0 = 1.2$, $\epsilon = 0.3$, $\omega = 0.4$ and $\theta = \pi/2$. These choices, as well as that for L , are motivated mainly by the results of the observations by Kontoyiannis and Watts (1994) and of the numerical simulations by Dimas and Triantafylou (1995). Namely, the most unstable waves produced in the latter work compare very well with the observations of the former, which show wavelengths of 260 Km, periods of ~ 8 days, e-folding space and time scales of 250 Km and 3 days respectively. In our case, since the downstream speed was set to 1 m/s , our e-folding time scale would correspond, in dimensional units, to approximately 3.5 days. The flow field resulting from the time dependent version of (2) is shown in fig. 2 for three different subsequent time snapshots $t = 0$, $(T/2)$ (fig. 2a), $t = T/4$ (fig. 2b) and $t = 3T/4$ (fig. 2c). Our system shows two different separatrices with a spatial periodic structure (see fig. 2), North and South of the jet. At small ϵ one has chaotic motion around them but without meridional mixing. In order to have a “large scale chaos”, i.e. the possibility that a test particle passes from North to South (and viceversa), crossing the jet, one needs the *overlapping of the resonances* (Chirikov 1979) $\epsilon > \epsilon_c$. In our case $\epsilon > \epsilon_c$ and ϵ_c depends on ω (in fig. 3 we show ϵ_c vs ω for our system).

The lagrangian motion of a test particle is formally a Hamiltonian system whose Hamiltonian is the stream function ϕ . If $\phi = \phi_0(x, y) + \delta\phi(x, y, t)$, where $\delta\phi(x, y, t) = O(\epsilon)$ is a periodic function of t , there exists a well known technique, due to Poincaré and Melnikov, which allows to prove whether the motion is chaotic (LL92). Basically if the steady part $\phi_0(x, y)$ of the stream functions admits homoclinic (or heteroclinic) orbits, i.e. separatrices, then the motion is usually chaotic in a small region around the separatrices for small values of ϵ .

In S92 the Melnikov integral has been computed explicitly for the ϕ_0 and $\delta\phi$ that we have used in this paper, and thus proved the existence of lagrangian chaos. However, even if the Melnikov method can determine if the lagrangian motion is chaotic, it is not powerful enough for the study of other interesting properties which will be the focus of section 4.1.

Alternatively (or jointly), mixing in the flow field (2) can be created by adding a turbulent diffusion term. This was done utilizing a stochastic model for particle motion belonging to the category of the so-called "random flight" models (e.g. Thomson, 1987), which can be seen as simple examples of a more general class of stochastic models which can be nonlinear and have arbitrary dimensions, described by the generalized Langevin equations (Risken, 1989; for a review, see Pope, 1994):

$$ds_i = h_i(\mathbf{s}, t)dt + g_{i,j}(\mathbf{s}, t)d\mu_j \quad [i = 1, \dots, N] \quad (5)$$

where $\mathbf{s} = (s_1, \dots, s_N)$ are N stochastic variables which, in our context, are the turbulent velocity fluctuations, μ_i is a random process with independent increments, and h_i and $g_{i,j}$ are continuous functions. A general, remarkable characteristic of these models is their markovian nature, which obviously has a particular interest for this investigation. The theoretical motivation for the choice of markovian models to describe mesoscale ocean turbulence has been thoroughly discussed in Zambianchi and Griffa (1994a), Griffa (1996) and Lacorata et al. (1996); it is worth adding that this particular model has proved to accurately represent upper ocean turbulence in regions characterized by homogeneity and stationarity (see Zambianchi and Griffa, 1994b; Griffa et al., 1995; Bauer et al., 1997; but also the results of numerical simulations by Verron and Nguyen, 1989; Yeung and Pope, 1989; Davis, 1991), and is easily extended to more complex situations (van Dop et al., 1985; Thomson, 1986).

In our simulations, a turbulent velocity $\delta\mathbf{u}^{(T)}(\mathbf{x}, t)$ is added to the large-scale velocity field $\mathbf{u}^{(M)}(\mathbf{x}, t)$ resulting from the streamfunction (2). The resulting equation for the particle trajectory is:

$$\frac{d\mathbf{x}}{dt} = \mathbf{u}(\mathbf{x}, t) \quad (6)$$

where $\mathbf{u}(\mathbf{x}, t)$ is given by

$$\mathbf{u}(\mathbf{x}, t) = \mathbf{u}^{(M)}(\mathbf{x}, t) + \delta\mathbf{u}^{(T)}(\mathbf{x}, t). \quad (7)$$

Our model assumes $\delta \mathbf{u}^{(T)}(\mathbf{x}, t)$ as a Gaussian process with zero mean and correlation:

$$\langle \delta u_i^{(T)}(\mathbf{x}, t) \delta u_j^{(T)}(\mathbf{x}', t') \rangle = 2 \sigma^2 \delta_{ij} \delta(\mathbf{x} - \mathbf{x}') e^{-|t-t'|/\tau}. \quad (8)$$

With this choice, $\delta \mathbf{u}^{(T)}(\mathbf{x}, t)$ is a linear in time markovian process: the turbulent field is entirely described in terms of two parameters: the variance of the small scale velocity σ^2 and the e-folding time scale of the velocity auto-correlation function, i.e. its typical correlation time scale τ , which represents the time step of the markovian process. The interdependence among smaller and larger time scales of the lagrangian motion will be investigated in the following chapters.

3 The Markovian approximation

The idea to use stochastic processes to study (and describe) chaotic behaviour is rather old (Chirikov 1979, Benettin 1984). One of the most relevant and successful approach is the symbolic dynamic, which allows to give a detailed description of the statistical properties of a chaotic system in terms of a suitable discrete stochastic process (Beck and Schögl 1993).

Given a discrete dynamical system:

$$\mathbf{x}_t = S^t \mathbf{x}_0, \quad (9)$$

one can introduce a partition \mathcal{A} dividing the phase space in A_1, A_2, \dots, A_N disjoint sets (with $A_i \cap A_j = 0$ if $i \neq j$). From each initial condition one has a trajectory:

$$\mathbf{x}_0, \mathbf{x}_1, \dots, \mathbf{x}_n, \dots \quad (10)$$

The point $\mathbf{x}_0 \in A_{i_0}$ will select the integer i_0 , the next one $\mathbf{x}_1 \in A_{i_1}$ the integer i_1 and so on. Therefore for any initial condition \mathbf{x}_0 we have a certain symbol sequence:

$$\mathbf{x}_0 \rightarrow (i_0, i_1, \dots, i_n, \dots). \quad (11)$$

Now the study of the *coarse grained* properties of the chaotic trajectories is reduced to the statistical features of the discrete stochastic process $(i_0, i_1, \dots, i_n, \dots)$. A useful and important characterization of the properties of symbolic sequences is the Kolmogorov-Sinai entropy, defined by:

$$h_{KS} = \lim_{n \rightarrow \infty} (H_{n+1} - H_n), \quad (12)$$

with

$$H_n = \sup_{\{\mathcal{A}\}} \left[- \sum_{C_n} P(C_n) \ln P(C_n) \right], \quad (13)$$

and

$$C_n = (i_0, i_1, \dots, i_{n-1}), \quad (14)$$

where $P(C_n)$ is the probability of the sequence C_n and $\{\mathcal{A}\}$ is the set of all possible partitions.

We note that, from a theoretical point of view, the sup in (13) hides a very subtle point: sometimes there exist a particular partition, called *generating partition*, for which one has automatically the sup. A partition is generating if the infinite symbol sequence $i_0, i_1, \dots, i_n, \dots$ uniquely determines the initial value \mathbf{x}_0 . Unfortunately it is not trivial at all to know if a system possesses a generating partition. Moreover in practical applications, even if the system admits a generating partition, it is extremely hard to find it (see Beck and Schögl 1993 for more detail).

A part the difficulties for the choice of a suitable partition, the stochastic process given by the symbol dynamics with a given partition can have rather nontrivial features. Of course the optimal case is when the symbolic stochastic process is a Markov chain, i.e. the probability to be in the cell A_i at time t depend only on the cell at time $t - 1$. In this case is possible to derive all the statistical properties (e.g. entropy and correlation functions) from the transition matrix W_{ij} whose elements are the probabilities to have the system in the cell A_j at time t if at time $t - 1$ the system is in the cell A_i . See the Appendix for a summary of the properties of Markov chains.

Usually a k -order markovian process (i.e. one in which the probability to be in the cell A_j at time t depends only on the preceding k steps $t - 1, t - 2, \dots, t - k$), with large k , is necessary to mimic, with a good accuracy, a chaotic system. In particular by means of the quantities defined in eqs.

(12,13) and of consideration of information theory (see Khinchin 1957) we are able to estimate the order of the Markov process necessary to reproduce the statistics of the process $(i_0, i_1, \dots, i_n, \dots)$ generated by the dynamics. In fact it is possible to demonstrate (Khinchin 1957) that, defining

$$h_n = H_n - H_{n-1} \quad (15)$$

with H_{n-1} given by (13), if the process is a Markov process of order k then $h_n = h_{KS}$ for each $n \geq k + 1$. In the next section we apply this method, in our case, to give an estimate of the order k .

However we observe that usually it is relatively easy, using a markovian approximation of order $k \leq 4 \div 5$, to find a reasonable agreement for the K-S entropy (12) (or for the Lyapunov exponent). On the other hand for different properties, such as the correlation functions, it is necessary to use Markov processes of rather large order ($k \sim 8 \div 10$) just for a fair agreement.

The issue to mimic a low dimensional dynamical system in terms of a Markov process of a certain order is surely an interesting aspect in the field of chaotic dynamics but, in our opinion, with a weak relevance for many practical purposes in geophysics since one needs a very large statistics for the computation of the transition probabilities. Therefore we shall restrict our analysis to the simplest case of the approximation in terms of a Markov chain, i.e. a first order process. This practical approach has been successfully used in the study of certain problems related to the dynamical properties of small astronomical bodies such as comets (see Rickmann and Froeshlé, 1979 and Levinson 1991) and for the interpretation of geophysical phenomena (Fraedrich, 1988, Fraedrich and Müller, 1983).

We shall now explain how we proceeded to express the behaviour of our Gulf Stream-like system in terms of symbolic dynamics. First we reduced the ordinary differential equation (3) obtained by the stream function (2) to a discrete in time dynamical system, which was accomplished building the Poincaré map associated with (3). This represents an assessment of the possibility to write \mathbf{x}_{n+1} in terms of \mathbf{x}_n – defined as $\mathbf{x}_n = \mathbf{x}(t=nT)$ –:

$$\mathbf{x}_{n+1} = \mathbf{F}[\mathbf{x}_n]. \quad (16)$$

Writing down an explicit expression for $\mathbf{F}[\mathbf{x}_n]$ may be in general non trivial; however, it is worth noticing the importance the existence of such a relationship.

We have now to decide a suitable choice of the phase space partition. Differently from the case of the orbital evolution of comets, where the cells are rectangular regions of the phase space, for our system we shall adopt a partition whose cells have curved frontiers. Considering the streamline pattern of our flow field (fig. 2), the structure of the physical space accessible to fluid particles suggests an obvious, natural choice for the partition: a particle will find itself in state 1 when it is inside the jet core (open trajectories); states 2 and 3 correspond to trapping in the Northern and Southern recirculations respectively (closed trajectories) and states 4 and 5 to the far field, i.e. far from the jet (backward open trajectories).

This partition turns out to be particularly appropriate to describe some important mixing properties in our system, such as:

- (a) The residence times of particles in the trapping recirculations or inside the jet, which in the language of Markov chain (see Appendix) correspond to the first exit times from state i ($i = 1, \dots, 5$);
- (b) The meridional mixing times (MMT), i.e. the time it takes to a particle to enter the Northern (Southern) recirculation starting from the Southern (Northern) one, i.e. the time of first passage from cell 2 (3) to cell 3 (2);
- (c) The correlation function for a variable $\chi_i(n)$ which indicates if a determined state i is visited at time n (see below, eqs 23 and 24, and Appendix).

Because of the system symmetries, states 2 and 3 possess the same statistical properties and so do states 4 and 5; in particular, the following equalities hold:

$$W_{12} = W_{13}, \quad W_{23} = W_{32}, \quad W_{21} = W_{31}, \quad W_{22} = W_{33}, \quad \text{and so on} \quad (17)$$

Let us now describe how to compute statistics for the quantities (a,b,c). First of all, we can compute from a long trajectory $\mathbf{x}_0, \mathbf{x}_1, \dots, \mathbf{x}_n$ ($n \gg 1$) the transition probabilities:

$$W_{ij} = \lim_{n \rightarrow \infty} \frac{N_n(i, j)}{N_n(i)} \quad (18)$$

where $N_n(i)$ is the number of times that, along the trajectory, \mathbf{x}_t ($t < n$) visits the cell A_i and $N_n(i, j)$ is the number of times that $\mathbf{x}_t \in A_i$ and $\mathbf{x}_{t+1} \in A_j$. In table 1 we report the elements of the matrix.

Notice that, for each i :

$$\sum_j W_{ij} = 1 \quad (19)$$

We can express the probabilities $\{P_i\}$ in terms of the matrix $\{W_{ij}\}$:

$$P_i = \sum_j P_j W_{ji} \quad (20)$$

Let us stress that the eqs. (19, 20) hold even if the process is not a Markov chain. Under the assumption (approximation) that the symbolic stochastic process generated by our deterministic chaotic model is a Markov chain one can derive (see Appendix) the probability of the first exit times from state i in n steps:

$$P_i(n) = \left[\frac{(1 - W_{ii})}{W_{ii}} \right] (W_{ii})^n, \quad (21)$$

which is the statistics of residence times in state i . A slightly more complicated computation gives the probabilities $f_{ij}(n)$ of first passage from state i to state j in n steps:

$$f_{ij}(n) = (W^n)_{ij} - \sum_{k=1}^{n-1} f_{ij}(n-k)(W^k)_{jj}, \quad (22)$$

i.e. the statistics of the MMT. For the normalized correlation function $C_i(n)$ of the variable $\chi_i(n)$ defined as:

$$\chi_i(n) = \begin{cases} 1 & \text{if } \mathbf{x}_n \in A_i \\ 0 & \text{otherwise} \end{cases} \quad (23)$$

we have:

$$C_i(n) = ((W^n)_{ii} - P_i)/(1 - P_i). \quad (24)$$

The Kolmogorov-Sinai entropy for the Markov chain is nothing but the Shannon entropy for a Markov chain:

$$h_{KS} = h_S = - \sum_{i,j} P_i W_{ij} \ln W_{ij}. \quad (25)$$

Note that for a Markov process $h_n = H_n - H_{n-1} = h_{KS}$ for $n = 2$ (see above). Since the discrete time system is obtained looking it at times $0, T, 2T, \dots$ the Lyapunov exponent λ of the original system has to be compared with:

$$\lambda_M = \frac{h_S}{T}. \quad (26)$$

This last equation is easily understood noticing that h_{KS} gives the degree of information per step produced by the process, that for a chaotic system in two dimensions corresponds to the Lyapunov exponent apart from a time rescaling.

4 Numerical results

We now discuss the numerical results for the models introduced in section 2 and their comparison with the markovian approximation illustrated in section 3.

4.1 Mixing induced by chaotic advection

We first consider the deterministic model with the parameter B of the stream function eq. (2) varying periodically in time according to eq. (4) with the parameters $B_0 = 1.2$, $\epsilon = 0.3$, $\omega = 0.4$, $\phi = \pi/2$ and $c = 0.12$. With this choice the system is chaotic and exhibits mixing at large scale, i.e. North-South mixing occurs.

We show in fig. 4 the spreading at different times of a cloud of test particles. The domain is naturally defined from the basic cell that repeats itself creating a zonal periodic structure of wavelength L ; x thus varies in $[0, L]$, while y in $[-4, 4]$. We fixed *a posteriori* these bounds for y since for our choice of parameters no particles reach the far field, and no trajectories attains values in $|y|$ larger than $|4|$ (even though, in general, we expect low but non zero frequencies for these states, see also S92).

In general, whether a North-South mixing happens or not depends sensibly on the values of ϵ and ω . Typically the system reveals a strong preference

to have a long residence times in the Northern or the Southern half of the domain with respect to the jet core. This peculiar feature will play an important role in the comparison with the markovian approximation.

The transition matrix elements W_{ij} and the visit probabilities $\{P_i\}$ are computed by means of eq. (18), looking at \mathbf{x} every period i.e. for $t = T, 2T, \dots$ where $T = 2\pi/\omega$, see table 1 and 2. At a first glance, we can see that the requested symmetry properties are respected (eq. 17).

Now in order to test whether the system is well approximated by a first order Markov process we compute exit times, correlation functions, meridional mixing times and Lyapunov exponent from the actual dynamics and compare them with the markovian predictions.

In fig. 5 we show the first exit time probability distributions for the states 1, 2 (3) and the corresponding markovian predictions. After stressing that the straight lines of fig. 5 are not to be confused with best-fit curves, we see that the agreement is good over a certain range both for state 1 and 2 (3). The agreement between the markovian predictions and the actual results is rather poor for small and very large exit times. The above behaviour shows that the markovian approximation cannot hold at small times since the details of the dynamics are strongly relevant. In the same way non trivial long time correlations cannot be accounted for in terms of a first order markovian process.

In fig. 6 we can see how the correlation functions of χ_i (see eqs. 23-24) for the state 1 and 2 (3) are just in vague agreement with the corresponding correlations obtained from the markovian process. The trajectories in the recirculations (i.e. states 2 and 3) appear to be much more auto-correlated than those in the jet. Therefore we deduce that the system, although chaotic, has a strong memory as to which half (North or South) of the spatial domain it is visiting. So the typical evolution is a "rebound game" between state 2 and the South half of the jet during a certain time interval; then it crosses the jet core and performs again the same pattern between state 3 and the North half of the jet, until it jumps back; and so on.

This is strikingly evident looking at the distribution probabilities of the meridional mixing times, in fact in this case the markovian approximation completely fails (fig. 7).

The markovian approximation leads to a clear disagreement in this case because it actually happens that when a tracer leaves a recirculation region, say in the South half, and goes into the jet, most of the time it returns back to

some other Southern close orbit rather than passing through the jet barrier, while in the first order Markov approximation it is not possible to explain such a strong memory effect. This feature is a clear indication that higher order Markov processes are necessary to describe the statistics produced by the dynamics. This is shown in fig. 8, where transitions between states 1 and 2, and 1 and 3, are compared: whereas in the first order markovian approximation (solid lines) a test particle jumps very often from North to South, the results of our numerical experiments show a stronger tendency for particles to keep being confined either between states 1 and 2 or between 1 and 3.

In order to quantify the relevance of the memory effects we computed the block entropies h_n , defined in section 3 (eq. 15) at varying n . In fig. 9 we can see that to obtain the convergence of the entropies we need at least of a Markov approximation of order $6 \div 7$.

The Lyapunov exponent computed with a standard algorithm (see Benettin et al. 1980) is $\lambda = 0.05$, the first order Markov approximation gives $\lambda_M = 0.03$, while the extrapolation with the asymptotic value $h = \lim_{n \rightarrow \infty} h_n$ gives $\tilde{\lambda}_M = 0.03$. The fact that $\tilde{\lambda}_M < \lambda$ is probably due to the fact that the partition here used is not a generating one (see section 3) however there exist a fair agreement between $\tilde{\lambda}_M$ and λ . It is worth noticing that the above features are fairly robust, and do not vary in a relevant way after weak changes of parameters.

4.2 Mixing induced by turbulent diffusion

Now we perform the same investigation discussed in the previous subsection setting $\epsilon = 0$ and turning on turbulent diffusion which is described in terms of a stochastic model for particle motion:

$$\frac{dx}{dt} = u + \eta_1, \quad \frac{dy}{dt} = v + \eta_2, \quad (27)$$

where u, v are given by the stream function (2) and η_i are zero mean gaussian stochastic processes with $\langle \eta_i(t) \eta_j(t') \rangle = \sigma^2 \delta_{ij} \exp[-|t-t'|/\tau]$. The gaussian variable η_i are generated by a Langevin equation (Chandrasekhar, 1943):

$$\frac{d\eta_i}{dt} = -\frac{\eta_i}{\tau} + \sqrt{\frac{2\sigma^2}{\tau}} \zeta_i, \quad i = 1, 2 \quad (28)$$

where the variables ζ_i are zero mean Gaussian noises with $\langle \zeta_i(t)\zeta_j(t') \rangle = \delta_{ij}\delta(t-t')$. The numerical integration of the equations has been performed by means of a stochastic 4-th order Runge-Kutta algorithm (Mannella et al., 1989).

Now the motion is unbounded for the presence of the isotropic diffusive terms, so we need a “trick” to limit the dispersion along y inside a domain as similar as possible to the previous one. In this way we can hope to look for a transition matrix comparable with that one obtained in the chaotic deterministic case and compare the two models.

Since the chaotic model does not fill the states 4 and 5, we impose that if a tracer enters a backward motion region it is reflected back by changing the sign of the meridional turbulent velocity, being the stream lines in these regions almost parallel to the x direction. Let us stress that this boundary condition practically does not affect the mixing processes between the jet and the recirculation regions, therefore we simply need to follow only those branches of trajectory which fall within the domain of study and not the large scale diffusion motion far from the stream frame.

In the diffusive case we fix the values $\sigma = 0.05$ and $\tau = T/4$ as representative of an observable situation (see DGO93) and compute again the transition matrix and stationary frequencies of the 5 states (see tables 1 and 2).

In fig. 10 we show the spreading of a cloud of test particles. Notice that the artifact introduced to bound the dynamics in the y direction does not produce any artificial accumulation of particles near the boundary.

At first we notice that the elements of the transition matrix are close to those of the chaotic case. We have computed the transition probabilities over a time period T as for the chaotic case so that we can reasonably compare the two cases.

Fig. 11 shows the probabilities of the first exit times of the states 1, 2 and 3 and the relative markovian predictions. These distributions are very well approximated by the first order Markov process.

The correlation functions are shown in Fig. 12. The difference between the actual and the markovian curves is now smaller than in the chaotic case because of the presence of diffusion that decreases sensibly the degree of memory.

The most relevant difference with respect to the chaotic model is a clear improvement in the agreement with the markovian approximation for the

distributions of the meridional mixing times, see fig. 13. The memory effects are now smoothened by diffusion, and the transition rates are much more representative of the actual dynamics. Thus we can conclude that in the diffusive model the markovian approximation works much better than in the chaotic one. Looking at the block entropies h_n (15) we have a clear indication that the process is of a lower order respect the chaotic case (compare fig. 14 with fig. 9)

Just like in the previous case we have investigated the behaviour of the system varying the parameters σ and τ . We have observed that if we keep the quantity $\sigma^2\tau$ constant the system displays similar behaviours, even if the extent of the agreement between simulation results and markovian approximation slightly differs for different values of the turbulence parameters; this can be understood if we recognize that $\sigma^2\tau$ corresponds to the diffusion coefficient (see, e.g., Zambianchi and Griffa, 1994a). It has been shown that varying σ and τ even if keeping the diffusion coefficient constant can indeed affect the quantitative estimates of dispersion in cases characterized by inhomogeneity and/or nonstationarity (see, again, Zambianchi and Griffa, 1994a). On the other hand, the qualitative functional behaviour of the dispersion processes has been seen to be influenced very little by such changes in the parameters of turbulence (Lacorata et al., 1996).

4.3 Mixing jointly induced by chaotic advection and turbulent diffusion

A detailed analysis of Lagrangian data from the ocean aimed at determining contemporary presence and relative importance of chaotic and turbulent mixing is at present still lacking, as it would imply the evaluation of both one- and two-particle statistics parameters, which has been done only in the context of purely diffusive particle exchange investigations (see, e.g., Poulain and Niiler, 1989). However, in the real ocean we expect both the above mixing mechanisms, discussed in sect. 2, to be present at the same time.

One of the interesting results of the previous sections is not only the fact that one can look at particle exchange in terms of markovian processes, but also that the sampling time suitable for the description of chaotic and

turbulent exchange are of the same order of magnitude for fairly realistic simulations. This suggests the feasibility of a numerical experiment in which a stochastic term is added to a time dependent large-scale velocity field.

In addition, in the Introduction we mentioned the issue of a possible inconsistency of kinematic models as to the lack of lagrangian conservation of quantities such as potential vorticity. This difficulty, which has been discussed at length recently for two-dimensional chaotic flows (see, above all, Brown and Samelson, 1994; Balasuriya and Jones, 1996), is overcome in the combination of the two mixing processes, as turbulent diffusion can be seen as a sort of dissipation, which therefore acts so as to “smear” potential vorticity gradients.

In this numerical experiment we use the model equations (6, 7) with $\mathbf{u}^{(M)}(\mathbf{x}, t)$ given by the stream function (2) with the time-dependent perturbation (4) and for the turbulent velocity $\delta\mathbf{u}^{(T)}(\mathbf{x}, t)$ we use the stochastic process defined in eqs. (27-28); the parameters are: $B_0 = 1.2$, $\epsilon = 0.3$, $\omega = 0.4$, $\theta = \pi/2$ and $\sigma = 0.05$, $\tau = T/4$ where $T = 2\pi/\omega$. As one can see this choice for the parameters is simply a superposition of the two previous cases.

Also in this case the matrix elements (i.e. the transition probabilities) are comparable with the other ones (see Table 1). As we can see from figs. 15 and 16 the distributions of the residence times and of the meridional mixing times display the same qualitative behaviour as the pure diffusive case (compare with figs. 11 and 13), from which we can deduce that for these features the most relevant effect is due to the diffusive term.

As to the correlation function (fig. 17) we note that there is a sensible improvement for the markovian approximation with respect to either the purely chaotic or the purely diffusive case, since the superposition of the two independent perturbations to the large scale flow strongly decreases the memory effects.

5 Discussion and conclusions

In this paper particle exchange in a meandering jet has been investigated by means of a kinematic model in which mixing is obtained by two different mechanisms: chaotic advection and turbulent diffusion. The large-scale

structure of the jet-like flow is assigned in terms of a stationary streamfunction. This has been modified in two ways, in order to provide the requested fluid exchange: chaotic advection is induced by adding a time-dependent, relatively small perturbation to the steady portion of the streamfunction. Alternatively, turbulent diffusion has been introduced by superimposing to this latter a stochastic field. The turbulent field has been selected so as to resemble as closely as possible the typical effect of upper ocean turbulence in the absence of coherent structures. Numerical simulations have been carried out for a case in which the two above effects have been jointly present, trying to take into account the richness and complexity of situations observed in the ocean, where the two different mixing mechanisms are thought to be present simultaneously, even if possibly acting at different time and space scales.

The intrinsically different nature of the two investigated mixing mechanisms has resulted in the past in disjointed descriptions of their respective effects: chaotic advection in correspondence in meandering jets has been studied, e.g., by means of methods derived from the dynamical systems theory (Pierrehumbert, 1991; S92; Wiggins, 1992; Duan and Wiggins, 1996), whereas the action of turbulent diffusion was clarified by phenomenological Lagrangian motion analysis (B91, DGO93).

In this paper mixing is studied in terms of particle transitions among areas of the physical two-dimensional space characterized by qualitatively different flow regimes, observed as realizations of a markovian process. Given the structure of the velocity field, the partition of the space accessible to particles is self-evident and physically consistent. A delicate point is obviously the choice of the appropriate scale for the sampling time of the process. However, in our cases an inherent time scale is present in the velocity field, and this is set by, in turn, either the space-time structure of the deterministic portion of the flow (chaotic case) or by the intrinsic memory time scale present in the stochastic velocity. The markovian approach results, in this sense, a quite natural one to undertake looking at the overall mixing from a unified perspective, embedding elements of dynamical systems and of stochastic process theory. Also, it is an alternative way to look at diffusion avoiding the usual diffusion coefficients, whose general relevance in geophysics has been recently subject to debate (see Artale et al. 1997 and Buffoni et al. 1997).

For some fluid exchange properties, the effects of the two above mixing mechanisms are comparable with the results of the markovian approximation: this is the case, for instance, of the exit times of particles from the

jet and the recirculating regions north and south of it. On the other hand, chaotic advection and turbulent diffusion act quite differently, under that perspective, when it comes to meridional mixing and correlation functions. The failure of the markovian approximation for the characterization of the meridional particle exchange in the chaotic is due to non-trivial long term memory effects. Since turbulent diffusion is modelled by a non-white noise process in the stochastic velocity field, we would expect for the turbulent case a closer behaviour to that predicted by the markovian approximation. For the same reason, given the results for the purely chaotic simulations, the combined effect of chaos and diffusion has been expected to be well described in markovian terms. This is indeed the case, and the results for the joint fluid exchange situations agree quite closely with the markovian predictions.

It is worth underlining that the possibility to look in terms of a markovian approximation at mixing in regions characterized by a quite complex flow structure, even in the presence of different transport mechanisms, can have quite interesting applicative consequences. When the small-scale details of mixing are beyond our interest, and if and when our flow system shows fairly well defined time scales, it is apparently possible to look at particle exchange in a relatively simple manner, over time scales which allow for a sensible reduction of the sampling rate. This aspect often turns out to be a critical constraint for the undertaking, e.g., of Lagrangian investigations of the real ocean, where reducing the required sampling rate can result in reducing the amount of data to be collected and transmitted.

6 Acknowledgements

We thank V. Artale and M. Falcioni for useful suggestions and first reading of the paper. GL would like to thank, also, the *Istituto di Fisica dell'Atmosfera* of CNR for hosting him while working on this paper. We are grateful to the ESF Scientific Programme TAO *Transport Processes in the Atmosphere and the Oceans* for providing meeting opportunities. This paper has been partly supported by INFM (Progetto di Ricerca Avanzato PRA-TURBO) and CNR (Progetto speciale coordinato *Variabilità e Predicibilità del Clima*).

Appendix

A Some properties of Markov chains

A Markov chain is a stochastic process in which the random variable describing the state of the system (in our case the cell occupied by the tracer) and the time are discrete and the probability to be in a given state at time n depends only on the state at time $n - 1$. All the properties of a Markov chain can be derived from the transition matrix, $\{W_{ij}\}$, whose elements are the probabilities to be in state j at some time n being at time $n - 1$ in state i . For example the probability to go to state j starting from i in n steps is simply:

$$Prob(i \rightarrow j; n) = (W^n)_{ij}. \quad (29)$$

An excellent introduction to Markov chain can be found in Feller (1968). In this appendix we only resume some formulas that are useful in describing some relevant properties of our system.

First of all we have:

$$\sum_j W_{ij} = 1. \quad (30)$$

In addition to matrix $\{W_{ij}\}$ one can compute the stationary probabilities P_i to visit the cells A_i as elements of the (left) eigenvector corresponding to the eigenvalue 1 :

$$P_j = \sum_i P_i W_{ij}, \quad (31)$$

Let us note that eqs. (30,31) are rather general results that hold for a generic discrete stochastic process. Eq. (30) describes the conservation of probability and eq. (31) is nothing but Bayes' Theorem. In order to have ergodicity and mixing properties the Markov chain must have a non zero probability to pass through any state in a finite number of steps, i.e. there exist a n such that $(W^n)_{ij} > 0$ (Feller 1968). Defining $\rho_i(t)$ the probabilities to visit the state i at time t , for a Markov chain we have:

$$\rho_j(t+1) = \sum_i \rho_i(t) W_{ij} \quad (32)$$

in this way we have the evolution of the probability vector ρ_i (see Rickman and Froeschlè, 1979), eq. (31) corresponds to $t \rightarrow \infty$ of eq. (32), i.e. the equilibrium distribution $\rho_i(\infty) = P_i$.

The probability of the first exit times from a state i can be simply defined as the probability to stay for $n - 1$ steps in state i times the probability to exit at step n , i.e.:

$$P_i(n) = (1 - W_{ii})(W_{ii})^{n-1}. \quad (33)$$

that can be rewritten as:

$$P_i(n) = \left[\frac{(1 - W_{ii})}{W_{ii}} \right] \exp(-n\alpha), \text{ with } \alpha = |\ln W_{ii}|. \quad (34)$$

In a similar way we can define the probability $f_{ij}(n)$ of the first arrival from state i to state j at step n . This is the probability to arrive to state j starting from i in n step i.e. $(W^n)_{ij}$ minus the probability of first arrival at step $n - k$ times the probability of return in k steps, i.e. $(W^k)_{jj}$ with $k = 1, \dots, n - 1$:

$$f_{ij}(n) = (W^n)_{ij} - \sum_{k=1}^{n-1} f_{ij}(n-k)(W^k)_{jj}. \quad (35)$$

For each state of a Markov process a correlation function can be defined for the variable $\chi_i(n)$ which is equal to 1 if at time n the i state is visited and to zero otherwise (see eqs. 23-24). The normalized correlation function

$$C_i(n) = \frac{\langle \chi_i(0)\chi_i(n) \rangle - \langle \chi_i(0) \rangle^2}{\langle \chi_i(0)^2 \rangle - \langle \chi_i(0) \rangle^2}. \quad (36)$$

is strictly related to the diagonal element $(W^n)_{ii}$ of the transition matrix to the n -th power and to the stationary frequency P_i . Notice that

$$\langle \chi_i(0) \rangle = P_i, \quad \langle \chi_i(0)^2 \rangle = P_i. \quad (37)$$

Furthermore, being P_i the probability that the initial state at $n = 0$ be i and $(W^n)_{ii}$ the probability to be in i again after n iterations, one has:

$$\langle \chi_i(0)\chi_i(n) \rangle = P_i \cdot (W^n)_{ii} \quad (38)$$

and therefore:

$$C_i(n) = ((W^n)_{ii} - P_i)/(1 - P_i) \quad (39)$$

References

- Artale V., G. Boffetta, A. Celani , M. Cencini and A. Vulpiani, 1997: Dispersion of passive tracers in closed basins: beyond the diffusion coefficient. *Phys. of Fluids*. **9**, 3162.
- Backus, R.H., 1986: Biogeographic boundaries in the open ocean, in *Pelagic Biogeography, UNESCO Tech. Pap. Mar. Sci.*, **49**, 9.
- Balasuriya, S. and C.K.R.T. Jones, 1997: Transport in barotropic jets via potential vorticity dissipation. to appear on *Phys. of Fluids*.
- Beck C. and F. Schlögl, 1993: *Thermodynamics of chaotic systems*. Cambridge University Press.
- Benettin G., 1984: Power-law behavior of Lyapunov exponents in some conservative dynamical systems. *Physica D* **13**, 211.
- Benettin G., L. Galgani, A. Giorgilli and J.M. Strelcyn, 1980: Lyapunov characteristic exponents for smooth dynamical systems and for Hamiltonian systems: a method for computing all of them. *Meccanica* **15**, 9.
- Bower A.S., 1991: A simple kinematic mechanism for mixing fluid parcels across a meandering jet. *J. Phys. Oceanogr.* **21**, 173.
- Bower A.S. and M.S. Lozier, 1994: A closer look at particle exchange in the Gulf Stream. *J. Phys. Oceanogr.* **24**, 1399.
- Bower A.S., H.T. Rossby, 1989: Evidence of cross-frontal exchange processes in the Gulf Stream based on isopycnal RAFOS float data. *J. Phys. Oceanogr.* **19**, 1177.
- Bower A.S., H.T. Rossby, J.T. Lillibridge, 1985: The Gulf Stream - barrier or blender?, *J. Phys. Oceanogr.* **15**, 24.
- Buffoni G., P. Falco, A. Griffa and E. Zambianchi, 1997: Dispersion processes and residence times in a semi-enclosed basin with recirculating gyres. The case of Tirrenian Sea. *J. Geophys. Res.* **102**, C8, 18699.

- Cecconi F. and A. Vulpiani, 1995: Approximation of chaotic systems in terms of markovian processes. *Phys. Lett. A* **201**, 326.
- Chandrasekhar S., 1943: Stochastic Problems in Physics and Astronomy. *Rev. of Mod. Phys.* **15**, 1.
- Chirikov B.V., 1979: A universal instability of many-dimensional oscillator systems. *Phys. Rep.* **52**, 263.
- Colin de Verdière A., 1983: Lagrangian eddy statistics from surface drifters in the Eastern North Atlantic, *J. Marine Res.* **41**, 375.
- Cornillon P., D. Evans and D. Large, 1986: Warm outbreaks of the Gulf Stream into the Sargasso Sea. *J. Geophys. Res.* **91**, 6583.
- Crisanti A., M. Falcioni, G. Paladin and A. Vulpiani, 1991: Lagrangian Chaos: Transport, Mixing and Diffusion in Fluids. *La Rivista del Nuovo Cimento* **14**, 1.
- Davis R.E., 1991: Observing the general circulation with floats. *Deep-Sea Res.* **38**, S531.
- Duan J. and S. Wiggins, 1996: Fluid exchange across a meandering jet with quasiperiodic variability. *J. Phys. Oceanogr.* **26**, 7, 1176.
- Dutkiewicz S., A. Griffa and D.B. Olson, 1993: Particle Diffusion in a Meandering Jet. *J. Geophys. Res.* **98**, 16487.
- Feller W., 1968: *An Introduction to Probability theory and its Applications, Vol. I*. Wiley, New York.
- Fraedrich K., 1988: El Niño/Southern Oscillation Predictability. *Monthly Weather Rev.* **116**, 1001.
- Fraedrich K. and K. Müller, 1983: On Single Station Forecasting: Sunshine and Rainfall Markov Chains. *Beitr. Phys. Atmosph.* **56**, 108.
- Griffa A., 1996: Applications of stochastic particle models to oceanographic problems, in R.J. Adler, P. Muller, B.L. Rozovskii (eds.), *Stochastic Modelling in Physical Oceanography*, Birkhäuser, Boston, 113.

- Griffa A., K. Owens, L. Piterbarg, B. Rozowskii, 1995: Estimates of turbulence parameters from Lagrangian data using a stochastic particle model. *J. Marine Res.* **53**, 371.
- Halliwell G.R. and C.N.K. Mooers, 1983: Meanders of the Gulf Stream downstream Cape Hatteras. *J. Phys. Oceanogr.* **14**, 1275.
- Khinchin A.I., 1957: *Mathematical Foundations of Information Theory*. Dover Publications, New York.
- Kluiving R., H.W. Capel, R.A. Pasmarter, 1992: Symbolic dynamics of fully developed chaos I. *Physica A* **183**, 67.
- Kontoyiannis H. and D.R. Watts, 1994: Observations on the variability of the Gulf Stream path between 74W and 70W. *J. Phys. Oceanogr.* **24**, 1999.
- Krauss W., C.W. Böning, 1987: Lagrangian properties of eddy fields in the northern North Atlantic as deduced from satellite-tracked buoys. *J. Marine Res.* **45**, 259.
- Lacorata G., R. Purini, A. Vulpiani and E. Zambianchi, 1996: Dispersion of passive tracers in model flows: effects of the parametrization of small-scale processes. *Ann. Geophysicae.* **14**, 476.
- Lee T., 1994: Variability of the Gulf Stream path observed from satellite infrared images. Ph.D. dissertation, University of Rhode Island, 188 pp.
- Lichtenberg A.J. and M.A. Lieberman, 1992: *Regular and Chaotic Dynamics*, Springer-Verlag.
- Levinson H.F., 1991: The long-term dynamical behavior of small bodies in the Kuiper belt. *Astr. Jour.* **102**, 787.
- Mannella R. and V. Palleschi, 1989: Fast and precise algorithm for computer simulation of stochastic differential equations. *Phys. Rev.* **A40**, 3381.
- Nicolis C., W. Ebeling and C. Baraldi, 1997: Markov processes, dynamic entropies and statistical prediction of mesoscale weather regimes. *Tellus* **49A**, 108.

- Pope S.B., 1994: Lagrangian PDF methods for turbulent flows. *Ann. Rev. Fluid Mech.* **26**, 24.
- Rickman H. and C. Froeschlè, 1979: Orbital evolution of short-period comets treated as a Markov process. *Astr. Jour.* **84**, 1910.
- Risken H., 1989: *The Fokker-Planck Equation*. Springer, Berlin, pp. 472.
- Samelson R.M., 1992: Fluid exchange across a meandering Jet. *J. Phys. Oceanogr.* **22**, 431.
- Samelson R.M., 1996: Chaotic transport by mesoscale motions, in R.J. Adler, P. Muller, B.L. Rozovskii (eds.), *Stochastic Modelling in Physical Oceanography*, Birkhäuser, Boston, 423.
- Thomson D.J., 1984: Random walk modelling of diffusion in inhomogeneous turbulence. *Quart. J.R. Met. Soc.* **110**, 1107.
- Thomson D.J., 1986: A random walk model of dispersion in turbulent flows and its application to dispersion in a valley, *Quat. J. R. Met. Soc* **112**, 511.
- Thomson D.J., 1987: Criteria for the selection of stochastic models of particle trajectories in turbulent flows. *J. Fluid Mech.* **180**, 529.
- Tracey K.L. and D.R. Watts, 1986: On Gulf Stream meander characteristics near Cape Hatteras. *J. Geophys. Res.* **91**, 7587.
- van Dop H., F.T.M. Nieuwstadt, J.C.R. Hunt, 1985: Random walk models for particle displacements in inhomogeneous unsteady turbulent flows. *Phys. Fluids* **28**, 1639.
- Vazquez J. and D.R. Watts, 1985: Observations on the propagation, growth and predictability of Gulf Stream meanders. *J. Geophys. Res.* **90**, 7143.
- Verron J., K.D. Nguyen, 1989: Lagrangian diffusivity estimates from a gyre-scale numerical experiment on float tracking, *Oc. Acta* **12**, 2, 167.
- Watts D.R., 1983: Gulf Stream variability, in A. Robinson (ed.), *Eddies in Marine Science*, Springer Verlag, Berlin, 114.

- Wiggins S., 1992: *Chaotic transport in dynamical systems*. Springer, Berlin, pp. 352.
- Yang H., 1996: Chaotic transport and mixing by ocean gyre circulation, in R.J. Adler, P. Muller, B.L. Rozovskii (eds.), *Stochastic Modelling in Physical Oceanography*, Birkhäuser, Boston, 439.
- Yeung P.K., S.B. Pope, 1989: Lagrangian statistics from direct numerical simulations of isotropic turbulence. *J. Fluid Mech.* **207**, 531.
- Zambianchi E., A. Griffa, 1994a: Effects of finite scales of turbulence on dispersion estimates. *J. Mar. Res.* **52**, 129.
- Zambianchi E., A. Griffa, 1994b: On the applicability of a stochastic model for particle motion to drifter data in the Brazil/Malvinas extension, *Annali Ist. Univ. Navale* **LXI**, 75.

TABLES

Table 1
Transition matrix elements

W_{ij}	Case A	Case B	Case C
W_{11}	.66	.74	.58
W_{12}	.17	.13	.21
W_{13}	.17	.13	.21
W_{21}	.12	.09	.14
W_{22}	.88	.91	.86
W_{23}	.00	.00	.00
W_{31}	.12	.09	.14
W_{32}	.00	.00	.00
W_{33}	.88	.91	.86

Table 2
Visit probabilities

P_i	Case A	Case B	Case C
P_1	.26	.25	.25
P_2	.37	.375	.375
P_3	.37	.375	.375

Case A - Deterministic chaotic model defined by eq. (3) related to the stream function (2) with parameters $L = 7.5$, $B_0 = 1.2$, $c = 0.12$, $\omega = 0.4$, $\epsilon = 0.3$.

Case B - Turbulent diffusion model defined by eqs. (27-28) with parameters $\sigma = .05$ $\tau = T/4$.

Case C - Model with chaotic advection plus turbulent diffusion with the same parameters of case A and B.

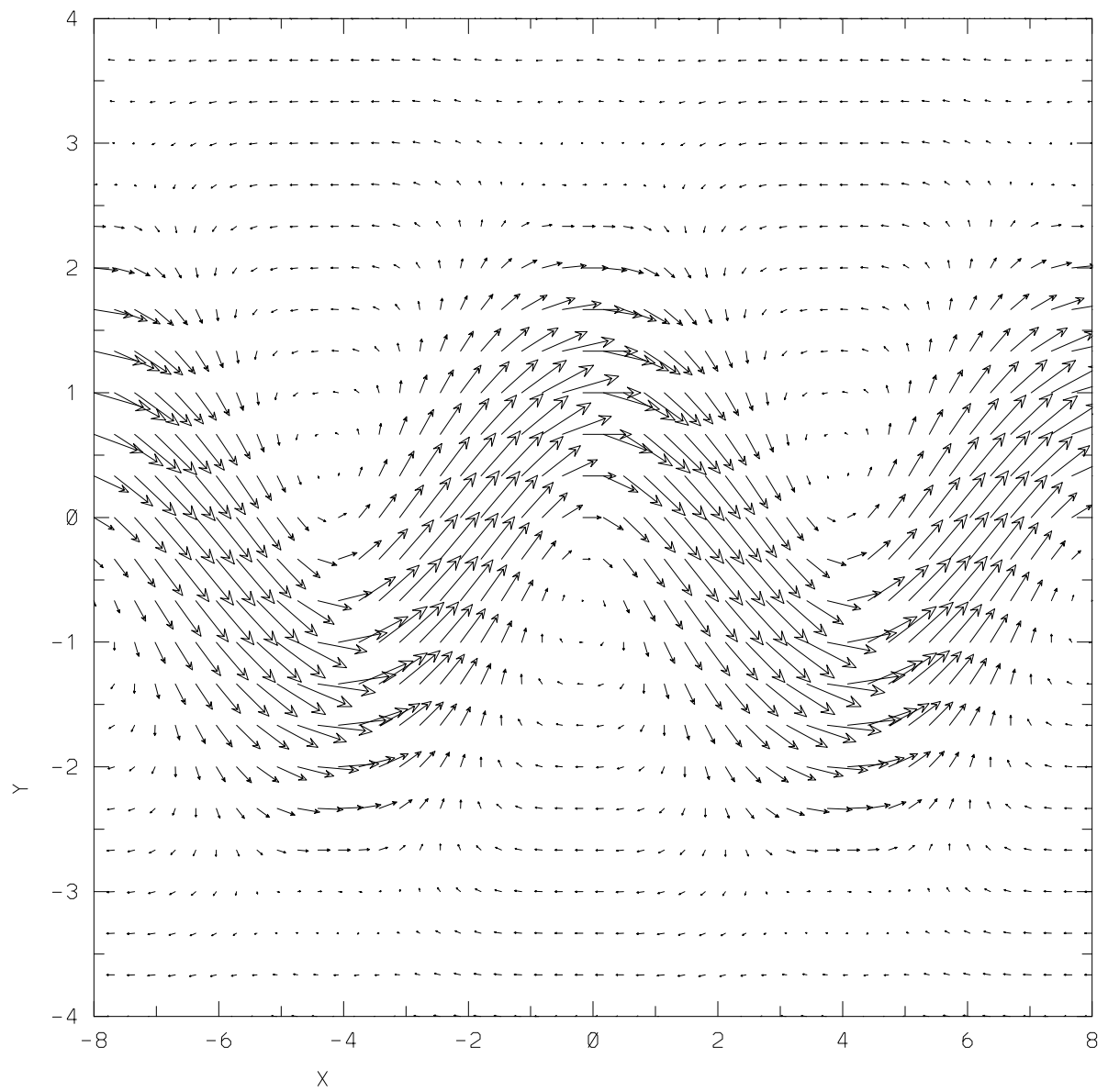
The statistics have been computed over $2 \cdot 10^6$ periods.

FIGURE CAPTIONS

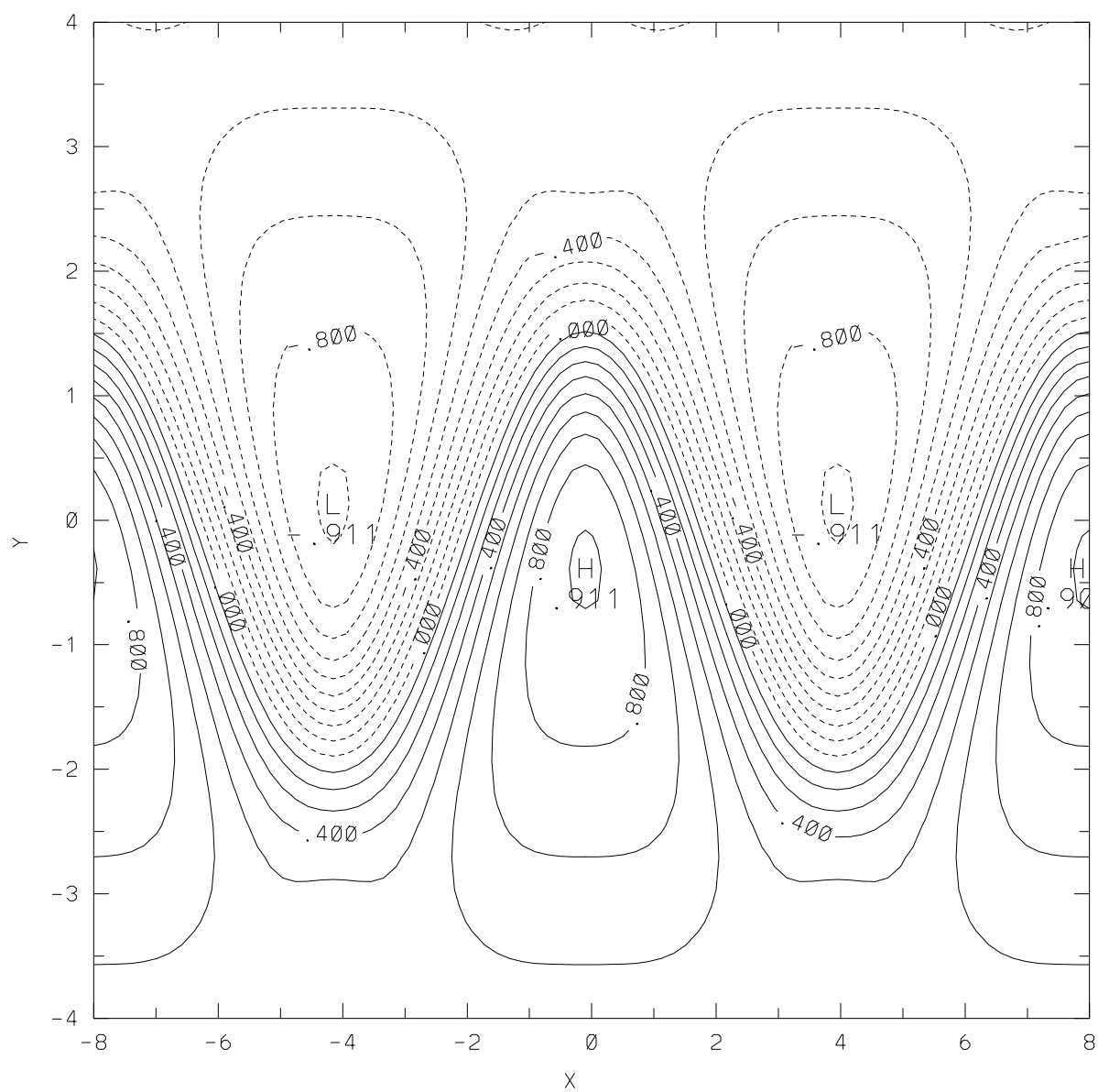
- FIGURE 1: Snapshot of the velocity field derived from the stream function eq.(2) with $L = 7.5$, $B_0 = 1.2$, $c = 0.12$.
- FIGURE 2: Stream lines of the time-dependent stream function eq.(2), with B given by eq.(4), $B_0 = 1.2$, $\omega = 0.4$ and $\epsilon = 0.3$ ($T = 2\pi/\omega$), at three different times: (a) $t = 0$, ($T/2$), (b) $t = T/4$ and (c) $t = 3T/4$.
- FIGURE 3: Critical values of the periodic perturbation amplitude for the overlap of the resonances, ϵ_c/B_0 vs ω/ω_0 , for the stream function (2) with $L = 7.5$, $B_0 = 1.2$, $c = 0.12$ and $\omega_0 = .25$, which is the typical frequency for the rotation of a tracer on the boundary of the recirculation gyres. The critical values have been estimated following a cloud of 100 particles initially located between the states 1 and 2 up to 500 periods.
- FIGURE 4: Spreading of a cloud of 5000 tracers at different times for the deterministic model (see Fig. 2): (a) $t = 0$ all tracers are inside a very small square, (b) $t = T$, (c) $t = 5T$, (d) $t = 10T$, (e) $t = 20T$ and (f) $t = 100T$.
- FIGURE 5: Probability distribution of the first exit times from states 1 (diamonds), 2 (squares) and 3 (crosses) for the deterministic model (see Fig. 2). The straight lines are the markovian predictions given by eq.(33) with W_{ii} of table 1 (case A). The time unit is the period T of the perturbation. The statistics is computed over $2 \cdot 10^6$ periods.
- FIGURE 6: Correlation functions of the states 1 (diamonds) and 2 (crosses) compared with the markovian predictions (continuous lines) eq. (39) for the deterministic model (see Fig. 2).
- FIGURE 7: Probability distribution of the meridonal mixing times (MMT) compared with the markovian predictions (continuous lines) eq. (33) for the deterministic model (see Fig. 2).
- FIGURE 8: Comparison between the symbolic sequence of the states as function of time (for $t = T, 2T, \dots$) obtained by the integration of the deterministic model equations (1,2) (dotted lines) and the symbolic

sequence generated from the Markov chain (solid lines) defined by the transition matrix computed as described in eq.(18) and reported in table 1 (case A) . Here 0 represents the state 1 i.e. the jet while 1, -1 the recirculation gyres i.e. the states 2,3.

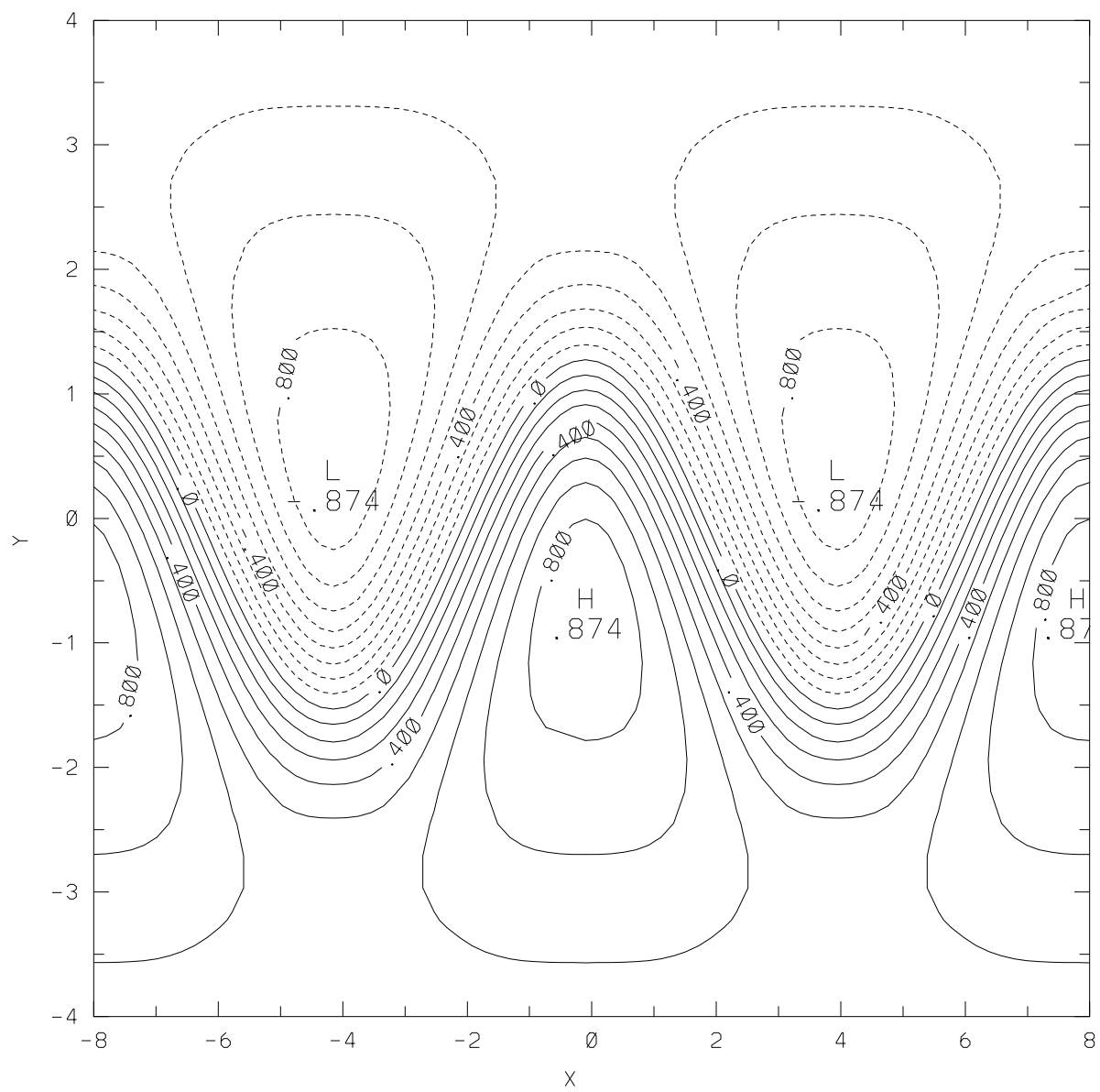
- FIGURE 9: Block entropies h_n vs n (15) for the deterministic model (see Fig. 2), computed from a sequence of 10^6 symbols.
- FIGURE 10: The same as figure 4 for the stochastic model given by eqs.(27,28), with parameters $\sigma = 0.05$ and $\tau = T/4$. The time unit T is set equal to the period of the deterministic perturbation (see Fig. 2).
- FIGURE 11: Probability distribution of the first exit times from states 1,2 and 3 for the stochastic model (see Fig. 10). The straight lines are the markovian predictions given by eq.(33) with W_{ii} of table 1 (case B).
- FIGURE 12: Correlation functions compared with the markovian predictions (continuous lines) eq. (39) for the stochastic model (see Fig. 10).
- FIGURE 13: Probability distribution of the MMT compared with the markovian predictions eq. (35) for the stochastic model (see Fig. 10).
- FIGURE 14: Block entropies h_n vs n for the stochastic model, computed from a sequence of 10^6 symbols.
- FIGURE 15: Probability distributions of the first exit times from states 1,2 and 3 in the model with chaotic advection combined with turbulent diffusion (sect. 4.3) with parameters: $B_0 = 1.2$, $\omega = 0.4$, $\epsilon = 0.3$ and $\sigma = 0.05$, $\tau = T/4$ where $T = 2\pi/\omega$. The straight lines are the markovian predictions given by eq. (33) with W_{ii} of table 1 (case C).
- FIGURE 16: Probability distributions of the MMT compared with the markovian predictions eq.(35) for the model and the parameters of figure 15.
- FIGURE 17: Correlation functions compared with the markovian predictions eq.(39) for the model and the parameters of figure 15.



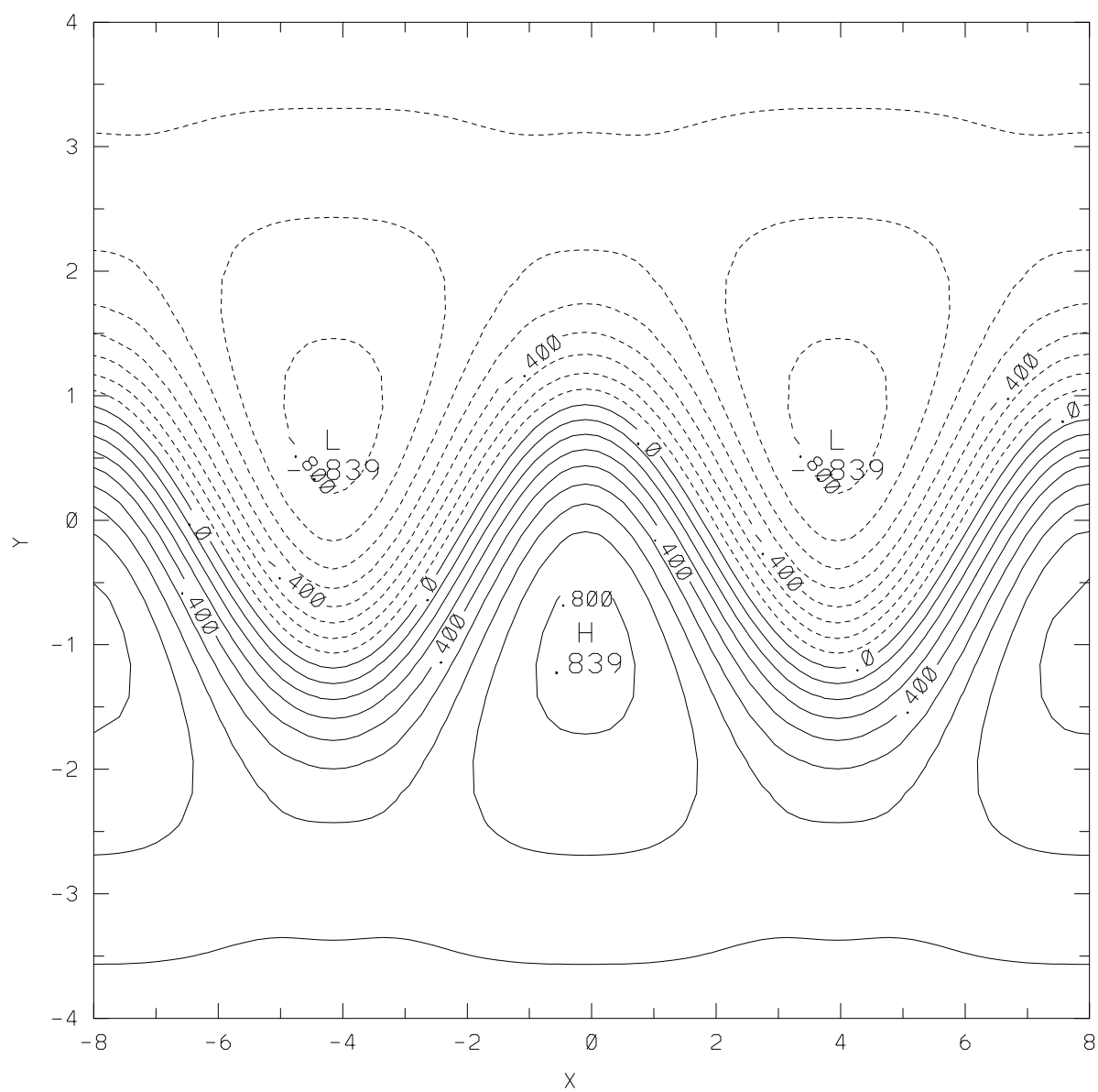
$.919\text{E}+00$
→
MAXIMUM VECTOR



CONTOUR FROM -.90000 TO .90000 CONTOUR INTERVAL OF .10000 PT(3,3)= .60931



CONTOUR FROM -.80000 TO .80000 CONTOUR INTERVAL OF .10000 PT(3,3)= .60922



CONTOUR FROM $-.80000$ TO $.80000$ CONTOUR INTERVAL OF $.10000$ PT(3,3)= $.60906$

